Article:
Palacios, A and Bradley, D (2022) Hydrogen and wood-burning stoves. Philosophical Transactions of the Royal Society A: Mathematical, Physical and Engineering Sciences, 380 (2221). 20210139. ISSN 1364-503X

https://doi.org/10.1098/rsta.2021.0139

PHILOSOPHICAL TRANSACTIONS A

Phil. Trans. R. Soc. A.

doi:10.1098/not yet assigned

Hydrogen and Wood-burning Stoves

Adriana Palacios[a,*], Derek Bradley[b]

[a]*Fundacion Universidad de las Americas Puebla, Department of Chemical, Food and Environmental Engineering, Puebla 72810, Mexico, ORCID ID "0000-0002-6972-5988".*
[b]*University of Leeds, School of Mechanical Engineering, Leeds LS2 9JT, UK.*

Keywords: hydrogen; wood stoves; decarbonisation; CO; particulates; blow-off.

Summary

Wood burning stoves, in Kenya and Mexico, are reviewed. With a Kenyan stove, burning charcoal, only 24% of the energy released reached the cooking pot. Initially, the proportion of CO in the leaving gases was 3%. Indoor concentrations of particulate matter (<2.5 μm diameter) can be abnormally high near a stove. Decarbonisation, by using H_2, is facilitated by a distribution system. Replacement by H_2, would ultimately rest upon wind, or water power, or it being a by-product in the production of heavier hydrocarbons from CH_4. The averaged burning rate in the Kenyan stove was 10 kW, over 20 minutes, with an initial peak value of about 30 kW. A possible replacement is a hob, composed of an array of small diameter H_2 jet flames. As an example, combustion of a 2 mm internal diameter H_2 jet flame, with a H_2 exit velocity of 27.2 m/s, would release 0.84 kW. Bearing in mind its improved efficiency, a single compact hob with an array of about 10 jets would suffice. A difficulty is the low mass specific energy of H_2. H_2 has a high acoustic velocity, and both high velocity subsonic combustion, and blending with natural gas, are briefly discussed.

1. Introduction

Wood burning stoves are widespread for heating and cooking, but they are usually inefficient, and lead to emissions of greenhouse gases GHG, and CO, as well as of harmful fine particulates. The paper first reviews data, from wood burning stoves (including charcoal) in Africa and Mexico. Their performances can certainly be improved, but after this review, decarbonisation is discussed, in terms of substituting wood-burning stoves with compact arrays of small hydrogen fuel jets. The H_2 can originate from both water and wind power, or by H_2, formed as a by-product during manufacture of heavier hydrocarbons.

An array of small H_2 jet flames would appear to be one alternative. There are a variety of combustion

*Author for correspondence (adriana.palacios@udlap.mx).

†Present address: Chemical, Food and Environmental Engineering

Universidad de las Americas Puebla, Puebla, 72810, Mexico

regimes within which lifted H_2 jet flames can be generated. The regimes can be defined by two dimensionless groups. One is the laminar flame thickness of the H_2/air mixture normalised by the exit diameter of the H_2 jet pipe. The other is the flow number, U^*, partly comprised of the ratio of the fuel jet velocity to the maximum laminar burning velocity. Diagrams with these two groups as axes can indicate a low velocity, laminar flame, quench limit, and, at higher values of U^*, a jet flame blow-off limit [1].

Hydrogen has a high acoustic velocity, which at the higher subsonic Mach numbers, in contrast to the low velocity oven jet flames, facilitates the generation of high heat release rates. A regime of supersonic flows can also be identified. The regime diagram is shown to be practically useful in identifying suitable operational modes for blended fuels, such as H_2/CH_4.

2. Characteristics of Wood-Burning Stoves

Data on traditional Africa stoves are rather sparse, but some valuable data are available [2], providing information on the performance of a typical stove. Repercussions are reviewed in [3] and cover the related global warming and particulate emissions. It is concluded in [3] that a meal cooked with charcoal creates 2-10 times, and in the case of fire wood, 5-16 times, the global warming that would be created if the same meal were to be cooked using kerosene or liquid petroleum gas, LPG. However, although charcoal is worse than other fuels with respect to GHG emissions, it can lead to reductions in concentrations of particulate matter. Such concentrations, from households using charcoal, were about 88% lower than those using open wood fires. Charcoal created 465 $\mu g/m^3$; and open wood fires 3764 $\mu g/m^3$. Health data over a period of years from Kenyan families, using both wood and charcoal showed that charcoal users experienced 44-65 percent fewer cases of acute lower respiratory infections.

In Mexico, approximately 25% of the homes use firewood as the main energy source. In rural communities, it is the main source of energy. Valuable data on particulate pollution in Mexico appear in [4]. The impact of wood burning stoves on indoor air pollution was measured. Concentrations of indoor particulate matter (diameter < 2.5 μm), were 693 $\mu g/m^3$ close to the stove, 658 $\mu g/m^3$ in the kitchen, away from the stove, and 94 $\mu g/m^3$, in the patio. An improved design of stove reduced the concentration near the stove by 71%. The US National Ambient Air Quality Standards in $\mu g/m^3$, for outdoor 24-hour levels, at that time, was 65 $\mu g/m^3$.

3. Performance of an African Charcoal-Burning Stove

The performance characteristics of a Kenyan charcoal stove, of the type sold in local markets, was suitably instrumented and enclosed. This was in order to facilitate measurements of gas flows, as described in [2]. The cooking vessel, through which water flowed, was the heated medium. It was of 170 mm diameter and 50 mm height. The heating stove, containing the fuel, operated in a batch-like mode, and was of 227 mm diameter, sealed at the bottom, with a height of 132 mm. Air flow rates were continually metered, as 0.5 kg of the different charcoals were burned, over a period of about 30 minutes, with a constant air flow rate.

Flows of exhausting O_2, CO, and CO_2 were metered continually, and their % mole fraction concentrations are plotted against time in Fig. 1(a), which is reproduced from [2].

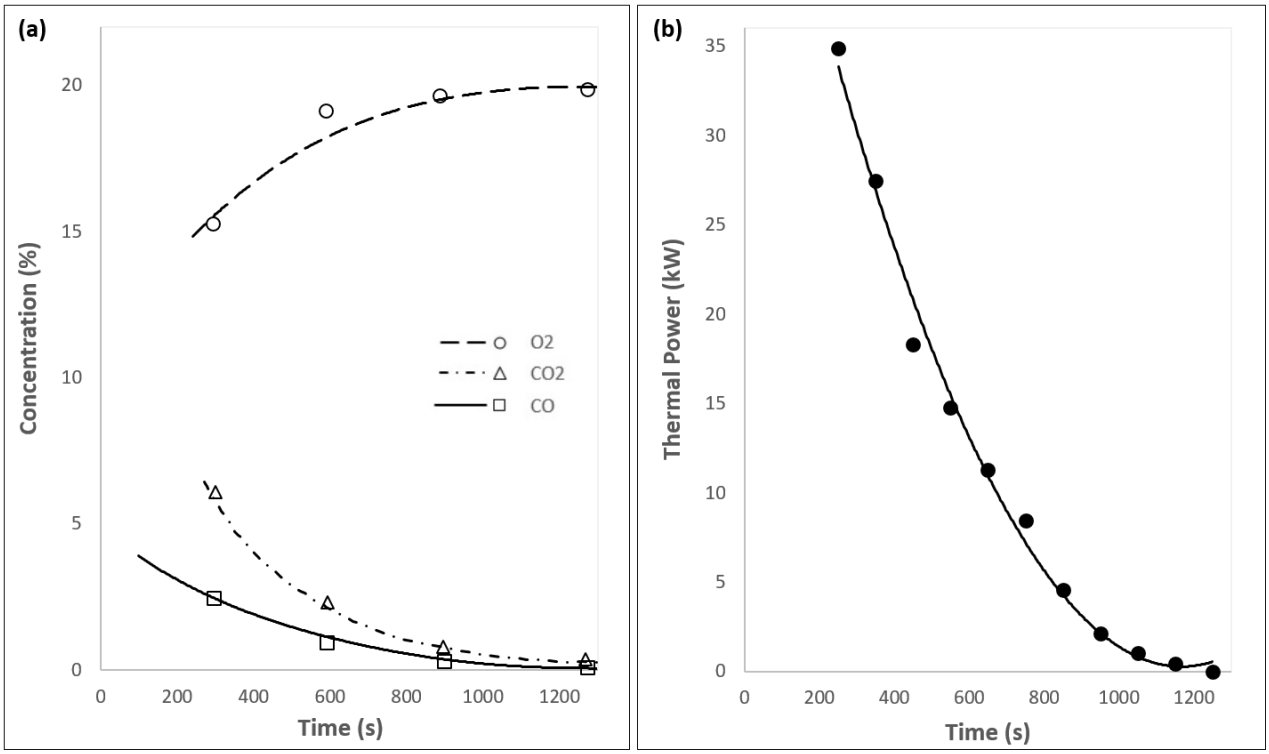

Figure 1. (a) Gas mole fractions of gases, when burning Wood Charcoal, derived from wattle and acacia. Reproduced from [2]. Fig. 1 (b) Thermal power during burning. Variation of heat release rate with time, during charcoal combustion.

Towards the end of combustion, the proportion of O_2, measured with a Beckman Model 715 Monitor, reached a maximum of about 20%. Prior to that, the concentration was reduced below this value by combustion. This reduction can be seen in Fig. 1(a). The reduction in O_2 concentration at any instant was assumed to be directly proportional to the heat release rate, in kW. The overall integration of these O_2 deficit values with respect to the time is assumed to be proportional to the overall heat release. The constant of proportionality was evaluated from the overall heat release, as measured by the amount of charcoal consumed. In the present case, this was 453 kg, with an overall heat of reaction of 12.33 MJ. The constant of proportionality was evaluated, and the derived variation of heat release rate, in kW, with time, is plotted in Fig. 1(b).

It was found that only 23.6% of the energy release reached the cooking pot. There was some improvement in efficiency when the heating stove was modified to allow the circulation, of the incoming air around it, in order to preheat it, prior to combustion. Mexican studies have also demonstrated significant increases in the efficiency of stoves to be possible, with improvements of from 30 to 60% [5]. A further possibility for improved performance could result from the recovery of some of the low-grade heat in the exhausting gases, through installing a heat exchanger.

Even with the normal ventilation of a room, the CO concentration could become dangerously high, and stoves should not be introduced into houses, unless the exhausting gas is led to a chimney. The initial burning period is particularly noxious. Potential radical decarbonisation changes do no not preclude improvements to wood stoves in the interim.

4. Jet Flame Heat Release Rates on a Burner

4.1. Combustion Regimes

Decarbonisation is proposed, through the replacement of wood-burning stoves by more compact arrays of efficient, small hydrogen fuel jets arranged in hobs. The design of such burners rests upon the results of studies of burning fuel jets, involving mathematical modelling and experiments [1,6]. As a result of these studies, the two key dimensionless groups emerged. One was δ_k/D, the thickness of a laminar flame of the fuel/air mixture, δ_k, at its maximum burning velocity, S_L, normalised by the fuel pipe diameter, D, at the exit plane. The other group involved the fuel jet velocity, u, at the exit plane, within a flow number, $U^*=(u/S_L)(\delta_k/D)^{0.4}(P_i/P_a)$. The last term is the ratio of the initial stagnation to the atmospheric pressure.

Because of the importance of the δ_k/D group in jet flame design, an accurate value for δ_k is necessary and, despite some inevitable problems in the case of H_2, the expression of Göttgens et al. [7] was chosen, with:

$$\delta_k = (k/Cp)T_o/(\rho_u S_L). \quad (1)$$

This defines the thickness of an inner layer, which is controlled by the location of a temperature To, below which there is no reaction. The k, Cp and ρ_u variables are the thermal conductivity at To, the specific heat at constant pressure at To, and the density of the unburned gas, respectively. Necessary thermo-physical properties, throughout this paper, were obtained from the GasEq code [8].

Diagrammatic plots of δ_k/D against U^* facilitate the identification of different combustion regimes. This approach is particularly valuable for the present subsonic lifted jet flames. It was originally developed in [9] for the different combustion regimes that are identified in Fig. 2, covering a wider range of fuels, but here the figure is confined to H_2 jet flames, with pipe diameters of 1.5, 2 and 3 mm, and also a single 2 mm CH_4 jet flame. The last is included, because it is more typical of hydrocarbon flames than is H_2, and the two fuels are frequently blended. The black circles in the figure show blow-off limits for H_2/CH_4 blends. Above these values of U^*, the flame blows off the burner. Blow-off limits for CH_4 and H_2 flames are shown by the broken and full line boundary curves. Flame quench and choked flow limits of lifted flames also are shown.

The present study involves jet velocities at the pipe exit plane that range between 5 and 100 m/s. These velocities were found from the expression for the corresponding Mach numbers, M, with γ the ratio of specific heats, [10,11], namely:

$$M^2 = 2/(\gamma - 1)[(P_i/P_a)^{(\gamma - 1)/\gamma} - 1]. \quad (2)$$

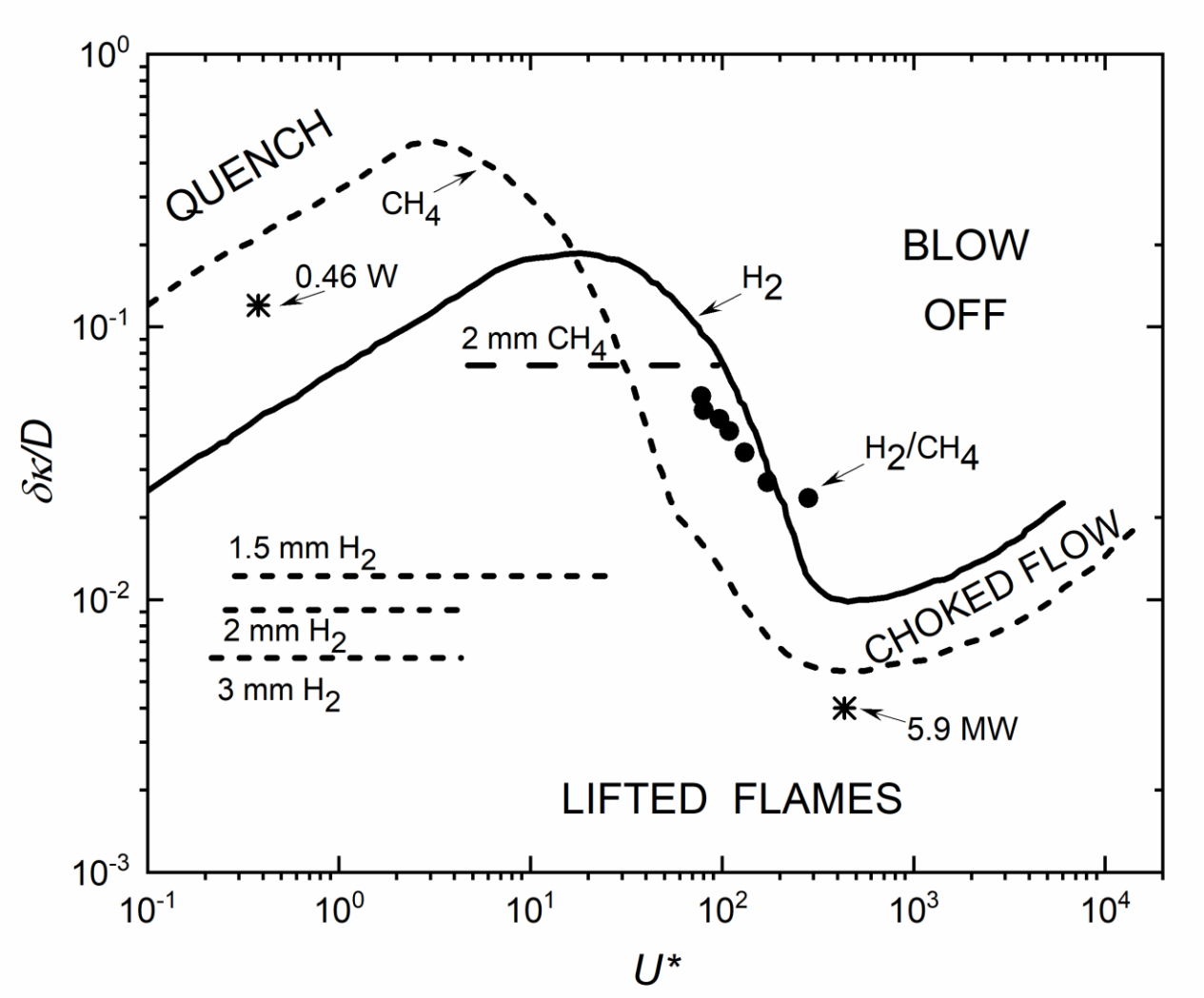

Figure 2. Four loci of jet flames in diagram of plots of δ_k/D against U^*.

The loci of three H_2 jet flames, with S_L= 2.99 m/s [12], that will be studied in detail, are shown by the three lower horizontal lines in Fig. 2. Such flames can exist between two limits, at lower and upper values of U^*. The lower limit is approached as a flame become weaker, ultimately culminating in a quenched laminar flame. In [13] is a report of a weak H_2 flame generated on a hypodermic needle with an inner diameter of 0.152 mm, and a fuel flow rate of 3.9 mg/s. The heat release rate is 0.46 W. The authors suggest this is the weakest flame ever observed. In terms of the present parameters δ_k/D=0.12, and U^* is 0.38. This point is marked by an asterisk, along with the heat release rate, in Fig. 2. It can be seen that the point lies between the quench curve for H_2 and that for CH_4. In another context, this phenomenon can be disadvantageous. Similar small diameter leakages can develop in pipes and an H_2, leakage night be ignited and the flame survive. The flame might be almost invisible and remain undetected.

The situation is different for the CH_4 flame, with its operational horizontal line in the upper part of Fig. 2, primarily as a result of its greater thickness, with δ_k/D=0.07219 and S_L=0.37 m/s [12]. This dashed line has U^* ranging from 4.70 to 95. But before the horizontal line operationally attains 95, it intersects the CH_4 blow-off curve at U^*=30, where u=31.7 m/s, and the jet flame blows-off at an upper U_b^* limit of 30.0, where u=31.7 m/s.

4.2. Thermal Power Characteristics of Hydrogen Jets

Figure 2 enables the operational regimes of practical jet flames to be selected. Having identified these different regime boundaries, it remains to evaluate the different jet flame heat release rates at different H_2

exit velocities from the pipes. This is repeated for pipes of different diameters. The heat of reaction for H_2 is 120 MJ/kg and this enabled the heat release rate of a flame to be calculated for the anchored flames at different values of u.

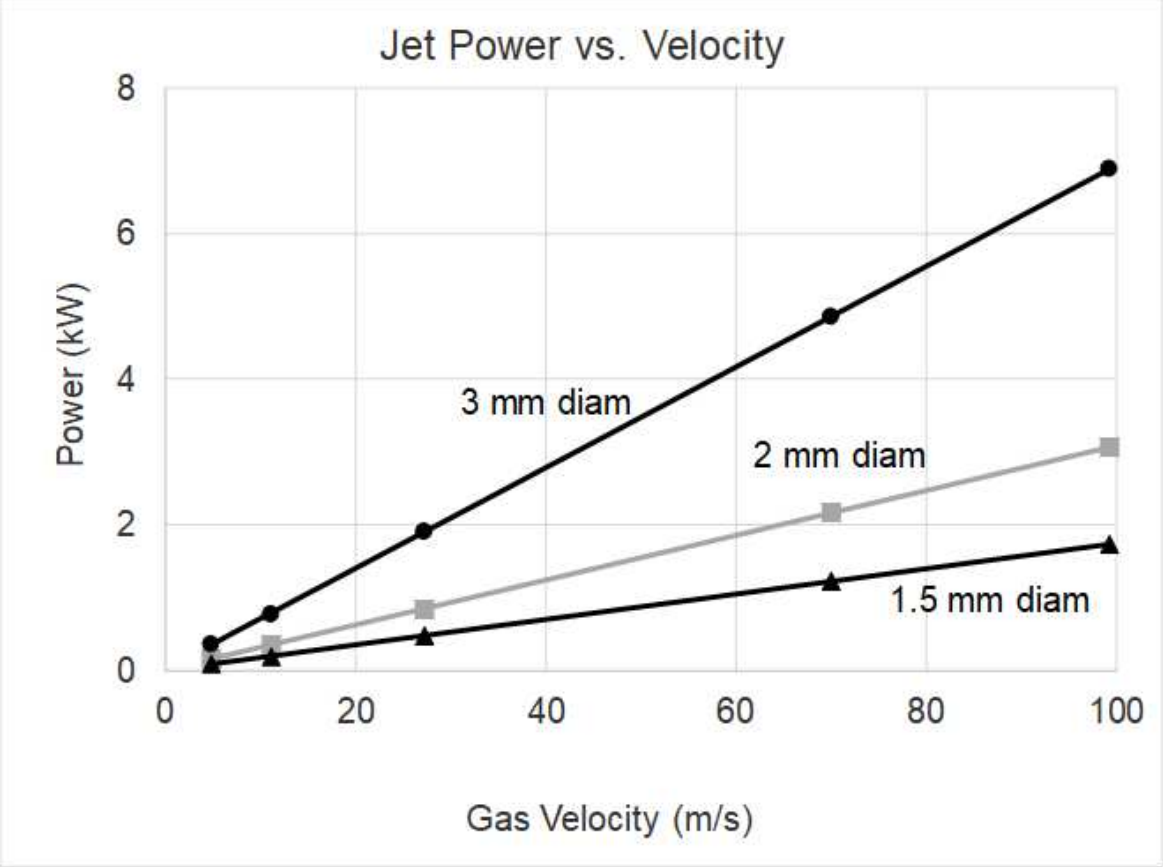

Figure 3. Thermal power variations with H_2 jet velocity for different pipe exit diameters.

The heat release rate variations with H_2 jet velocities, for the exit plane diameters that appear in Fig. 2, are shown in Fig. 3. The thermal powers of the jets increase linearly with the jet velocity, u. They increase, more sharply, the greater the jet diameter. Bearing in mind the limited length of burner flames, in practice a jet velocity of 20 m/s is more probable than one of 100 m/s.

The 2 mm diameter CH_4 lifted jet flame in Fig. 2, just prior to blow-off, attains a velocity of 31.7 m/s. With a heat of reaction of 50 MJ/kg for CH_4, this gives an associated heat release rate of 3.25 kW. It can be seen from Fig. 3 that to attain this power with a H_2 jet of the same diameter would require a jet velocity slightly in excess of the available 100 m/s. The lower heat release rate with H_2 arises from its mass specific energy density being lower than that of CH_4. This density is the product of the mass density and the heat of reaction/unit mass. The H_2/CH_4 ratio of mass densities is 0.1257, and that of the heats of reaction 2.4. This gives a H_2/CH_4 ratio of energy densities of 0.302.

Because of the inferior energy density of H_2 it was found that a 3.5 mm diameter pipe would be necessary for H_2, in order to attain the same heat release rate as that attained by CH_4 with a 2 mm pipe. Similarly, a 2 mm H_2 jet, with u=100 m/s, barely reached the heat release rate that prevailed just prior to CH_4 blow off, at 31.7 m/s, with the same diameter.

Another possible approach for enhancing the heat release rate might be to add air into the fuel supply pipe. Such additions of air have been studied experimentally in [14]. It was found that the air addition increased the value of the flow number at blow off, U_b^* in the case of C_3H_8, but decreased it when CH_4 was the fuel. This was mainly attributed to the significantly larger air requirement for the combustion of C_3H_8 being partially satisfied by the air addition, whereas in the case of that for CH_4 it was overly satisfied and the addition was without benefit. This dependency upon the necessary air requirement for a single mole of fuel, is expressed by f, the ratio of fuel to air moles at the equivalence ratio necessary for the attainment of maximum laminar burning velocity, S_L, of the fuel. Relevant values of f, from the experimental data in [9,12], are 0.046 for C_3H_8, 0.107 for CH_4 with, a high value of 0.81 for H_2, because of its very low air requirement. There would be no benefit in adding air to H_2.

4.3. Lift-Off Distance and Flame Height

The component flames in the array need to be appropriately compact. An attempt was made to estimate both the lift-off distance of the flame from pipe exit plane and the height of the flame**.** The flame lift-off distance, L, is an important jet flame characteristic, and not surprisingly, it also is dependent upon f. An expression for L/D, appropriate for subsonic H_2 jet flames, is given in [1], as a function of U^*:

$$(L/D)f = 0.11U^* - 0.2. \quad (3)$$

This expression for U^* does not employ δ_k to derive the flame thickness in the expression for U^* but, δ, which is derived from the kinematic viscosity of the mixture, divided by S_L. It readily can be shown that $U_\delta^*/U^* = (\delta/\delta_k)^{0.4}$, where U_δ^* employs δ. With this relationship, Eq. (3) becomes:

$$(L/D)f = 0.11U^*(\delta/\delta_k)^{0.4} - 0.2. \quad (4)$$

Some values of flame thicknesses are given in [9]. For H_2 flames $\delta_k/\delta = 4.56$, and $(\delta/\delta_k)^{0.4} = 0.545$. For the H_2 jet flame on a 2 mm pipe, with a high value of u=99.8 m/s, U^*=5.1, and, with f=0.81, Eq. (3) gives L/D=1.31. This yields a lift-off distance of 2.62 mm, creating a suitably compact flame. However, the high jet velocity of 100 m/s cannot be regarded as normal for a stove. A more typical value would be one of, say, 27 m/s. With a pipe diameter of 2 mm, this gives a small value of U_δ^*=1.03, for which the data in [1] suggest a very small value of L/D, giving a value of L in the region of 0.002 mm.

Predictions of the flame height present more problems than the more precisely definable lift-off distance. These are due to the extensive, yet uncertain, mixing of burned gas and air and the nature of the observed boundary. To mitigate this, in [1] thermocouple measurements were employed to define the plume edges by a temperature of 800K. Estimates were then made of reacting plume volumes, and values of flame surface densities were established. This enabled revised jet height to diameter ratios, h/d, to be evaluated as a function of U^*. It was found in [1] that for $U^*<10$:

$$h/d = 1.26U^*. \quad (5)$$

For the current values of U^*=1.03 (u=27 m/s) and U^*=5.1, (u=99.8 m/s), this yields respective values of h/d of 1.3 and 6.4, namely h, = 2.6 and 12.8 mm for the 2 mm pipe diameter. Because of the uncertainties in defining plume boundaries, these results can only be regarded as approximate estimates.

5. Discussion

Historically and regionally, wood-burning stoves have been associated with either a no cost, or a low cost, fuel. In Mexico, for nearly 16.4 million people, firewood is the only fuel for cooking. Others use it in combination with liquid petroleum gas. About 80% of the firewood is obtained from natural collection, and 20% from purchases. One result is deforestation and desertification of the soil [15]. The southern states of the country have no gas pipelines. Costs of H_2, as an alternative source of energy could be reduced were there to be piped distribution. Currently, fuel prices can vary by at least an order of magnitude, and can be prohibitive. Small domestic hob burners are comprised of an array of small jet burners with jet velocities possibly in the range of 20-35 m/s.

Concentration on these small-scale aspects of H_2 consumption should not detract from beneficial aspects of its larger scale usages in industry and transport. Its small laminar flame thickness is symptomatic of its reactivity. In addition, its high acoustic velocity ensures high subsonic flow velocities, at Mach numbers just less than unity. As a consequence, a high subsonic Mach number can generate both high velocities and associated high heat release rates. A high pipe diameter can avoid blow-off. A design example of a higher-powered jet is a 5.9 MW, 10 mm diameter H_2 flare. This is located in the high velocity regime of Fig. 2. It is a flare, proposed for H_2 disposal, in the event of a potentially large-scale generation of H_2, as a consequence of a nuclear reactor mishap [16].

Another important use of H_2 is as a blending fuel with CH_4. Just as the creation of GHG must be minimised in the production of H_2, this must also be considered in its blending with CH_4.

Figure 4 summarises some of the key aspects. It shows the full range of S_L values of all H_2/CH_4 blends, as measured by Erjiang Hu et al. [12]. These are plotted against H_f, which is the concentration of H_2 moles, as a fraction of the sum of those of H_2 and CH_4. The relatively large increase in S_L, and associated decrease in δ_k, decrease U^* and enhance stability. The contribution of H_2 to the overall heat release rate only begins to exceed that of CH_4 when H_f reaches 0.8.

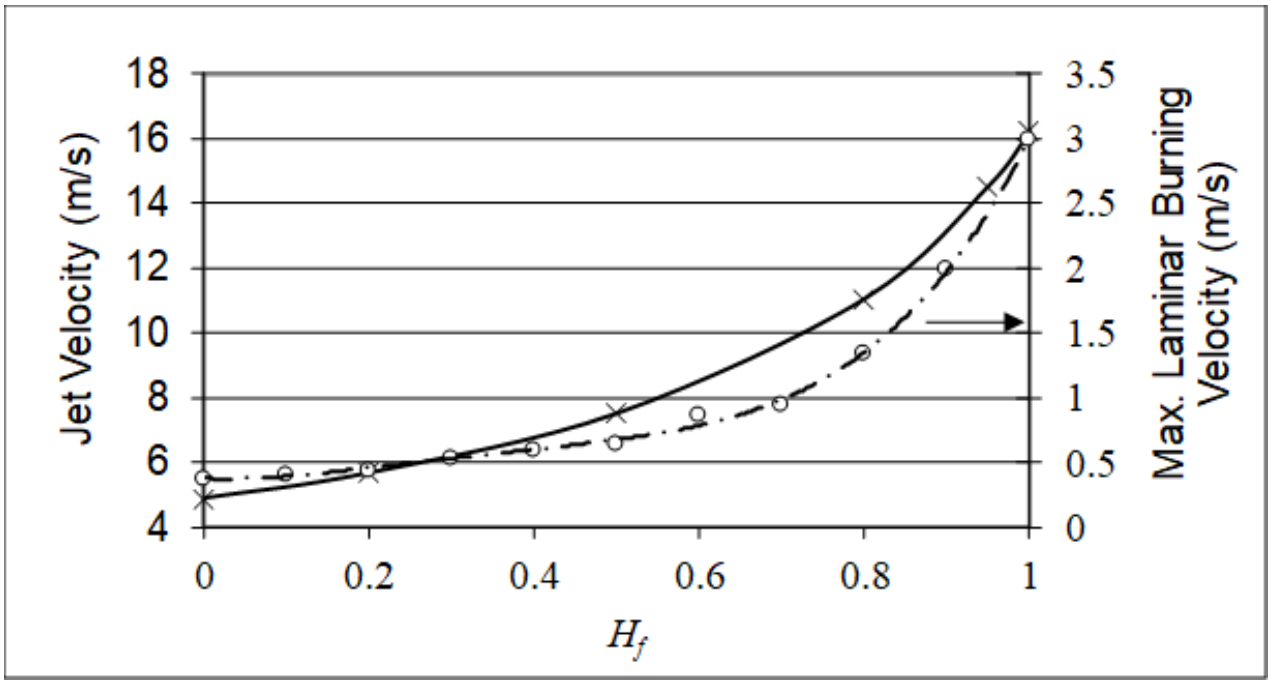

Figure. 4. (i) Variations in S_L for H_2/CH_4 blends [12] and (ii) jet velocity, u, to maintain a heat release rate of 0.5 kW. Pipe diameter = 2 mm.

The fuel blend jet velocity shows the increase in it that is necessary to maintain a power of 0.5 kW, regardless of H_f, with D=2 mm. This is a necessary consequence of the declining energy density, as H_f increases. Another interesting aspect, is that in the early stages of H_2 addition, up to about H_f=0.2, there is only a slight increase in the value of u that is necessary to maintain a constant power, close to the 0.5 kW, as can be seen from Fig. 4. This reduced sensitivity to a relatively low value of velocity makes this regime well suited to the economic substitution of CH_4 by H_2, without undue modification of the pipework. This is attractive, but the decarbonisation is minimal. Further details of these blended fuels are available in [17].

6. Conclusions

1. Changes in the overall heat release rate during the cycle of a charcoal-burning stove have been derived. These ranged from 35 kW at the start of the burn, which decayed to zero after 1200 s. Less than 23.6% of the total heat release was conveyed to the heated test pot.

2. If the stove is indoors, it can create dangerously high concentrations of both CO and small particulates.

3. A circular array of small lifted, H_2 jet flames, of but a few mm diameter, stable, and free of pollutants, could be a suitable alternative to wood-burning.

4. A disadvantage of H_2 is its relatively low specific energy, equal to 0.3 that of CH_4. Compensation for this can be through higher gas velocities and/or larger pipe diameters. There is no clear advantage in adding air to the fuel pipe.

5. Delays in implementing other potential decarbonisation changes do no not preclude improvements to wood stoves in the interim.

6. H_2 has an unusually high acoustic velocity. This can give high heat release rates at subsonic Mach numbers.

7. The generalised expression for the height of jet flames is insufficiently accurate. Allowance for the air requirement of the fuel is necessary.

8. Addition of a relatively small proportion of H_2 to natural gas by operating at H_f=0.2, produces minimal perturbation of the combustion. Further addition affects combustion, and can reduce the energy release significantly.

Authors' Contributions

AP and DB carried out 1) substantial contributions to conception and design, or acquisition of data, or analysis and interpretation of data; 2) drafting the article or revising it critically for important intellectual content; and 3) final approval of the version to be published.

Competing Interests

The authors declare that they have no competing interests.

References

1. Bradley D, Gaskell PH, Gu XJ, Palacios A. 2016. Jet flame heights, lift-off distances, and mean flame surface density for extensive ranges of fuels and flow rates. *Combust. Flame*. **164**, 400–409. (https://doi.org/10.1016/j.combustflame.2015.09.009).
2. Nyang'aya JA, Bradley D. 1985. The African charcoal stove: Its inefficiency and pollutants emission, *Kenya Jour. Sci. and Tech*. Series A **6**(1), 29–39.
3. Bailis R, Pennise D, Ezzati M, Kammen DM, Kituyi E. 2004. Impacts of greenhouse gas and particulate emissions from wood fuel production and end-use in sub-Saharan Africa. *University of Nairobi Research Archive*. (http://rael.berkeley.edu/old drupal/sites/default/files/very-old-site/OA5.1.pdf).
4. Zuk M, Rojas L, Blanco S, Serrano P, Cruz J, Angeles F, Tzintzun G, Armendariz C, Edwards RD, Johnson M, Riojas-Rodriguez H, Masera O. 2007. The impact of improved wood-burning stoves on fine particulate matter concentrations in rural Mexican homes. *J. Expo. Sci. Environ. Epidemio*. **17**, 224–232. (https://doi.org/10.1038/sj.jes.7500499).
5. Mexican Ministry of Environment and Natural Resources (SEMARNAT). 2016. Ecological saving stoves with chimney, environmental and health benefit for the population. (https://www.gob.mx/semarnat/articulos/estufas-ecologicas-ahorradoras-con-chimenea-beneficio-ambiental-y-de-salud-para-la-poblacion).
6. Bradley D, Gaskell PH, Gu XJ. 1998. The mathematical modelling of liftoff and blowoff of turbulent non-premixed methane jet flames at high strain rates. *Proc. Combust. Inst.* **27**, 1199–1206. (https://doi.org/10.1016/S0082-0784(98)80523-7).
7. Göttgens J, Mauss F, Peters N. 1992. Analytic approximations of burning velocities and flame thicknesses of lean hydrogen, methane, ethylene, ethane, acetylene and propane flames. *Proc. Combust. Inst*. **24**, 129–135. (https://doi.org/10.1016/S0082-0784(06)80020-2).
8. Morley C. 2021. GasEq: a chemical equilibrium program for windows. (http://www.gaseq.co.uk/).
9. Palacios A, Bradley D. 2017. Generalised correlations of blow-off and flame quenching for sub-sonic and choked jet flames. *Combust. Flame*. **185**, 309–318. (https://doi.org/10.1016/j.Combust, Flame. 2017.07.019).

10. Massey BS. 1989. Mechanics of fluids. 6th ed. US: Van Nostrand Reinhold (International).
11. Houghton EL, Brock AE. 1961. Tables for the flow of dry air. London: Edward R Arnold (Publishers).
12. Erjiang Hu, Zuohua Huang, Jiajia,He, Chun Jin,, Jianjun Zheng. 2009. Experimental and numerical study on laminar burning characteristics of premixed methane-hydrogen-air flames. *Int. Jour. of Hydrogen Energy.* **34**, 4876–4888. (https://doi.org/10.1016/j.ijhydene.2009.03.05812. 12).
13. Butler MS, Moran CW, Sunderland PB, Axelbaum RL. 2009. Limits for hydrogen leaks that can support stable flames. *Int. Jour. Hydrogen Energy* **34**, 5174–5182 (https://doi.org/10.1016/j.ijhydene.2009.04.012).
14. Palacios A, Bradley D, Hu L. 2016. Lift-off and blow-off of methane and propane subsonic vertical jet flames, with and without diluent air, *Fuel* **183**, 414–419. (https://doi.org/10.1016/j.fuel.2016.06.073).
15. Berrueta VM, Magallanes AB. 2013. Use of firewood in rural communities. Social Mexico. (https://www.mexicosocial.org/uso-de-lena-en-comunidades-rurales/).
16. Palacios A, Bradley D. 2020. Hydrogen generation, and its venting from nuclear reactors. *Fire Safety. Jour*. **113**, 102968. (https://doi.org/10.1016/j.firesaf.2020.102968).
17. Palacios A, Bradley D. 2021. Conversion of natural gas jet flame burners to hydrogen. *Int, Jour. Hydrogen Energy.* (https://doi.org/10.1016/j.ijhydene.2021.02.144).

Figure and table captions

Figure 1. (a) Gas mole fractions of gases, when burning Wood Charcoal, derived from wattle and acacia. Reproduced from [2]. Fig. 1. (b) Thermal power during burning. Variation of heat release rate with time, during charcoal combustion.

Figure 2. Four loci of jet flames in diagram of plots of δ_k/D against U^*.

Figure 3. Thermal power variations with H_2 jet velocity for different pipe exit diameters.

Figure. 4. (i) Variations in S_L for H_2/CH_4 blends [12] and (ii) jet velocity, u, to maintain a heat release rate of 0.5 kW. Pipe diameter = 2 mm.